UC Davis

UC Davis Previously Published Works

Title

Rapid assessment of drug response in cancer cells using microwell array and molecular imaging

Permalink

https://escholarship.org/uc/item/9vr3w8qw

Journal

Analytical and Bioanalytical Chemistry, 406(17)

ISSN

1618-2642

Authors

Wang, Min S
Luo, Zhen
Nitin, Nitin

Publication Date

2014-07-01

DOI

10.1007/s00216-014-7759-y

Peer reviewed

eScholarship.org Powered by the California Digital Library
University of California

Author Manuscript

Author Manuscript

Author Manuscript

Author Manuscript

HHS Public Access

Author manuscript

Anal Bioanal Chem. Author manuscript; available in PMC 2015 September 04.

Published in final edited form as:

Anal Bioanal Chem. 2014 July ; 406(17): 4195–4206. doi:10.1007/s00216-014-7759-y.

Rapid assessment of drug response in cancer cells using microwell array and molecular imaging

Min S. Wang,

Food Science and Technology Department, University of California, Davis, CA 95616, USA

Zhen Luo, and

Department of Biological and Agricultural Engineering, University of California, Davis, CA 95616, USA

Nitin Nitin

Food Science and Technology Department, University of California, Davis, CA 95616, USA

Department of Biological and Agricultural Engineering, University of California, Davis, CA 95616, USA

Abstract

Selection of personalized chemotherapy regimen for individual patients has significant potential to improve chemotherapy efficacy and to reduce the deleterious effects of ineffective chemotherapy drugs. In this study, a rapid and high-throughput in vitro drug response assay was developed using a combination of microwell array and molecular imaging. The microwell array provided high-throughput analysis of drug response, which was quantified based on the reduction in intracellular uptake (2-[*N*-(7-nitrobenz-2-oxa-1,3-diazol-4-yl)amino]-2-deoxy-D-glucose) (2-NBDG). Using this synergistic approach, the drug response measurement was completed within 4 h, and only a couple thousand cells were needed for quantification. The broader application of this microwell molecular imaging approach was demonstrated by evaluating the drug response of two cancer cell lines, cervical (HeLa) and bladder (5637) cancer cells, to two distinct classes of chemotherapy drugs (cisplatin and paclitaxel). This approach did not require an extended cell culturing period, and the quantification of cellular drug response was 4–16 times faster compared with other cell-microarray drug response studies. Moreover, this molecular imaging approach had comparable sensitivity to traditional cell viability assays, i.e., the MTT assay and propidium iodide labeling of cellular nuclei;and similar throughput results as flow cytometry using only 1,000–2,000 cells. Given the simplicity and robustness of this microwell molecular imaging approach, it is anticipated that the assay can be adapted to quantify drug responses in a wide range of cancer cells and drugs and translated to clinical settings for a rapid in vitro drug response using clinically isolated samples.

nnitin@ucdavis.edu.

Electronic supplementary material The online version of this article (doi:10.1007/s00216-014-7759-y) contains supplementary material, which is available to authorized users.

Author Manuscript Author Manuscript Author Manuscript Author Manuscript

Keywords

Microwell array; High throughput; Cancer; Drug response; Molecular imaging; 2-NBDG

Introduction

Currently, chemotherapy is one of the most commonly used methods to treat cancer [1], but the success of treating cancer using chemotherapy remains limited [1]. The major reasons for limited success with cancer chemotherapy are drug resistance and the lack of rational approaches to select optimal therapy for individual patients [1–3]. Therefore, to improve the success rate of cancer chemotherapy, it is necessary to have a rapid and sensitive assay to predict chemosensitivity of individual patients.

Chemotherapy sensitivity and resistance assays (CSRAs) are laboratory assays used for measuring the response of a patient's tumor tissue to selected chemotherapy drugs [4, 5]. In a typical CSRA, tumor tissues from patients are removed and cultured for a few days with selected chemotherapy drugs, and then assessed for cell death and survival [5]. From a laboratory viewpoint, CSRAs can provide predictive information regarding the chemosensitvity or chemoresistance of a patient's tumor to a given chemotherapy drug [6]. As such, CSRAs are recommended by the American Society of Clinical Oncologists for use in clinical trial settings [4, 6] as they have the potential to improve chemotherapy drug selection for individual patients. However, the use of CSRAs outside clinical trial settings is not recommended due to some inherent limitations and inconsistencies of the assays. These limitations include the extended culturing period of primary cells [4, 5], the lack of success in culturing cells from clinical samples [4], the requirement of a large sample, and the limited sensitivity to detect heterogeneity of cells in tumor tissue [3, 7], all of which could result in a delay in treating patients. Given these limitations, the integration of CSRAs into clinical settings has been limited thus far.

To better predict the drug response from a heterogeneous tumor sample, single cell microarray are well suited to be used for high-throughput quantification of drug response [8, 9]. The quantification of drug response using high-throughput cell microarrays have previously been demonstrated for liver [10], lung [11], and breast [12, 13] cancer cells. In these reports, microarrays of cancer cells were initially captured in microwell [12, 13] or spotted in a gel matrix [10] and cultured for 24–72 h prior to drug treatment. The drug response of cells in the microarray were measured after 12–48 h traditional assays such as immunofluorescence [10, 12] or Annexin V [13] labeling to evaluate cell viability and apoptosis. Despite achieving high throughput and potentially improving analysis of cellular heterogeneity in tumor cells, the current microarray assays require extended cell culturing period in a laboratory environment.

In this study, a rapid and high-throughput drug response assay was developed using a combination of microwell array and molecular imaging. The novelty of this current approach was based on (a) a rapid technique to capture cells uniformly inside individual microwells, (b) the evaluation of drug response of diverse cancer cells using multiple chemotherapy drugs, and (c) the rapid quantification of drug response of cancer cells after

Author Manuscript Author Manuscript Author Manuscript Author Manuscript

drug treatment based on the intracellular uptake of a glucose analog, (2-[*N*-(7-nitrobenz-2-oxa-1,3-diazol-4-yl)amino]-2-deoxy-D-glucose) (2-NBDG). Quantification of metabolic activity based on the intracellular 2-NBDG uptake was uniquely different from the conventional cell viability assays that include the methylthiazolyldiphenyl-tetrazolium bromide (MTT) assay [10] propidium iodide (PI) nuclear labeling of membrane permeabilized cells [13] and Annexin V labeling of damaged membrane [13]. It was also distinct from other microarray studies that used immunofluorescence to quantify the changes in gene [12] and cell surface marker [10, 11] expressions in response to drug treatments. 2-NBDG is a fluorescent analog of a PET tracer probe, 2-[^{18}F]-fluoro-2-deoxy-D-glucose with PET (FDG PET) that is clinically used for detection of tumors [14]. As cancer cells can metabolize glucose at a faster rate than normal cells [15, 16], the quantification of intracellular 2-NBDG uptake has been shown to be useful to evaluate drug response in cancer cells [17, 18].

Two cancer cell lines, HeLa (cervical) and 5637 (bladder) were used as model cell lines in this study to demonstrate the versatility of this assay for different cancers. Cisplatin and paclitaxel were chosen as model drugs in this study because both drugs are effective in treating a wide variety of cancers [19, 20] but has different cytotoxic mechanisms of action. Cisplatin belongs to the platinum-based anticancer drug class that forms adducts with DNA and subsequently blocks DNA replication in cells [19, 21]. Paclitaxel, on the other hand, is an antitumor drug that stabilizes microtubules, and thus prevents cell division [22, 23]. Quantification of the drug response at a single cell resolution using the combination of microwell array and molecular approach was 4 to 16 times faster compared with previous studies. The sensitivity of this approach was also compared with conventional flow cytometry and cell viability assays. Overall, the combination of cell microarray and molecular imaging using 2-NBDG illustrated the potential of this approach to rapidly quantify drug response of individual cells with high sensitivity and throughput.

Materials and methods

Materials

Human cervical carcinoma (HeLa), bladder cancer cells (5637) cells and MTT assay kit (30–1,010 K) were from ATCC (Manassas, VA). Dulbecco's modified Eagle's medium (DMEM), fetal bovine serum (FBS), trypsin/EDTA, penicillin–streptomycin (Pen-Strep), 2-NBDG, and PI were from Life Technologies (formerly Invitrogen, Carlsbad, CA). Dimethylsulfoxide (DMSO) and phosphate buffered saline (PBS) were from Thermo Fisher Scientific (Waltham, MA). Cisplatin and paclitaxel were from Sigma-Aldrich (St. Louis, MO). Poly(dimethylsiloxane) (PDMS) was from Dow Corning Corp. (Midland, MI). All chemicals and reagents are used as received unless otherwise specified.

Cells and cell culture

HeLa and 5637 cells were cultured in DMEM supplemented with 10 % FBS and 1 % Pen-Strep (complete DMEM) and maintained at 37 °C in a humidified atmosphere with 5 % CO_2 until they reached 90 % confluency. The cells were then detached from the flask using trypsin/EDTA, neutralized with complete DMEM and pelleted at 800 rpm for 2 min. The

Author Manuscript Author Manuscript Author Manuscript Author Manuscript

media was aspirated and cells were concentrated to between 0.5 and 1.0×10^6 cells/mL with complete DMEM.

Microwell array fabrication

A 100-μm size microwell array was fabricated as previously described [24]. Briefly, a silicon master mold of the microwell array design was drawn using an AutoCAD software (Autodesk, Inc. San Rafael, CA) and fabricated using standard photolithography by the Stanford Microfluidics Foundry. The microwell array was made by mixing the PDMS base and curing agent at a 10:1 (*w/w*) ratio and degassing the mixture for 15 min. Subsequently, the degassed PDMS was poured over the silicon mold and cured at 80 °C for 1 h. The cured PDMS was then affixed inside a 35×10 mm petri dish, treated with O_2 plasma to render the PMDS surface hydrophilic. Then a 1 % collagen solution was added to the microwell and placed under vacuum for 15 min to dislodge any trapped air bubbles inside the microwell. Collagen was used in this step to facilitate cell attachment to the microwells. The excess collagen was subsequently rinsed with ×1 PBS and dried using filtered compressed air before cell capturing (Electronic supplementary material, Fig. S1).

Capturing of cells in the microwell array

Cells were captured within the microwell array using a simple vacuum-assisted and sweeping method (supporting information). Briefly, an aliquot of cell suspension ($0.5–1.0\times10^6$ cells/mL) was added to the collagen-coated microwell array prepared above and placed under vacuum for 5 min to dislodge trapped air bubbles and to facilitate the entrance of cells into the microwell. Then, the cell-loaded microwell array was incubated at 37 °C in a humidified atmosphere with 5 % CO_2 for 30 min to allow the cells to attach to the microwell. After 30 min of incubation, excess cells outside the microwells were gently swept away using a clean coverslip (Electronic supplementary material, Fig. S1). The detached cells were removed by pipet, and the microwells were rinsed once with 1× PBS before use. A detailed schematic illustration of the microwell cell capturing method can be found in the Electronic supplementary material (Fig. S1).

Cisplatin and paclitaxel treatment of HeLa and 5637 cells inside the microwell

Stock solutions of cisplatin and paclitaxel were prepared in DMSO and were further diluted with complete DMEM before adding to the cells inside the microwells. The final concentrations of cisplatin and paclitaxel were 100 and 1 μM, respectively. The final DMSO concentration was 1 %, which had been shown to be nontoxic to HeLa [25] or 5637 [26] cells. The final drug concentrations used were within an order of magnitude of the LD_{50} values reported in other in vitro studies [26, 27]. HeLa cells were treated for 3 h for cisplatin and 2 h for paclitaxel; while the treatment time was 3 h with 5647 cells for both drugs. HeLa cells were only incubated with paclitaxel for 2 h because substantial cell detachment from the microwell was observed in 3 h. The cells in the microwells were kept at 37 °C in a humidified atmosphere with 5 % CO_2 during treatment (Fig. 1).

Author Manuscript Author Manuscript Author Manuscript Author Manuscript

Intracellular uptake of 2-NBDG by HeLa and 5637 cells inside the microwell

Stock solution (5 mg/mL) of 2-NBDG was prepared in water and added to the cells inside the microwell in complete DMEM immediately following drug treatment. The final concentration of 2-NBDG was 15 μg/mL for HeLa and 40 μg/mL for 5637 cells. These concentrations were selected based on the differences in baseline 2-NBDG uptake in the two different cell lines as determined by internal experiments (data not shown). After 30 min of incubation at 37 °C in a humidified atmosphere with 5 % CO_2, the 2-NBDG was aspirated and the microwells were washed twice with 1× PBS before imaging (Fig. 1).

Fluorescence microscopy

Fluorescence and brightfield images of the cells were taken using an Olympus IX-71 inverted fluorescence microscope with either a 4× or a 10× objective (Olympus UPlanFLN). The 2-NBDG was excited using a 100-W mercury arc lamp (OSHIO 102D) and a 480/30 nm excitation filter (Olympus), and the fluorescence emission was collected using a 590-nm long pass filter (590/70 nm, Olympus). The images were acquired using a Hamamatsu CCD camera with an exposure time of 200 ms. Three images from three independent experiments were acquired for each sample and thresholded to the same maxima and minima pixel intensities level.

Quantification of intracellular 2-NBDG

The integrated intensity of the intracellular 2-NBDG was quantified using the CellProfiler 2.0 (Broad Institute) [28]. The thresholded fluorescence images were uploaded into the CellProfiler pipeline and the Otsu Adpative threshold module was used to identify the cells on each image based on fluorescence intensity. In order to avoid background noise from cellular debris or overlapping cells from being analyzed, only the 10–40 pixel objects were considered as single cell and selected by the CellProfiler software. Then, the integrated intensity (intensity over area) of each selected cell was quantified using the CellProfiler software, and the mean integrated intensity of the drug-treated cells was normalized to that of the control cells.

Flow cytometry

For flow cytometry, the cells were cultured in a 6-well plate (Fisher) and grown to 80 % confluency. The media was removed and the cells were rinsed once with 1× PBS. The media was then replaced with either fresh complete DMEM (control) or chemotherapeutic drug diluted in complete DMEM. The drug treatment and intracellular 2-NBDG uptake steps were similar to the methods performed in the microwell array as described above. The cells in the plate were trypsinzed after 2-NBDG uptake and centrifuged to concentrate the cells to ~10^6 cells/mL. Intracellular 2-NBDG uptake and hence, labeling of the cells were analyzed using a BD FACScan flow cytometer at the UC Davis Comprehensive Cancer Center shared facility. A total of 20,000 events were counted for each sample, and the experiment was performed in triplicate. The geometric mean was used to determine the mean fluorescence intensity (MFI).

Author Manuscript Author Manuscript Author Manuscript Author Manuscript

Cell viability assay using the MTT assay

The MTT assay has been widely used to detect cell viability based on the reduction of soluble tetrazolium dye (yellow) to an insoluble formazan precipitate (purple) by metabolically active cells [29]. To access cell viability, HeLa and 5637 cells were grown on a 24-well plate until 90 % confluency. Then, 500 μL of either 100 μM cisplatin or 1 μM paclitaxel (pre-diluted with DMEM) were added to each well and incubated for 24 h in a 37 °C incubator supplemented with 5 % CO_2. Cells cultured under the same conditions but without any drug treatment were used as a control. After 24 h, 25 μL of the MTT substrate was added to each well and the plate was incubated for 3 h at 37 °C in the dark to reduce the MTT. Then, the plate was centrifuged at 4,000 rpm for 10 min to pellet the cells and solid formazan. The supernatant was removed and 250 μL DMSO was added to each well to solubilize the formazan crystals. After 10 min of incubation at 37 °C, 100 μL of the solubilized formazan was transferred to a fresh 96-well plate and the absorbance was measured at 540 nm. The absorbance was normalized to the control and presented as mean ±SD from five independent experiments.

Fluorescent live/dead assay with propidium iodide staining

The drug induced cell death of HeLa and 5637 cells were also evaluated optically using PI nuclear staining as described [30]. Briefly, cells were grown in an 8-well coverslip chamber until 70–80 % confluent to avoid overcrowding of cells in the 24-h assay. Then, 100 μM cisplatin or 1 μM paclitaxel (pre-diluted in complete DMEM) were added to each well and the cells were incubated for 3 and 24 h. After each incubation time point, the media were gently removed and replaced with 1× PBS. An aliquot of PI stain (5 μg/mL final concentration) was added to each well and incubated for 5 min in the dark before imaging. The percent cell death was determined by the ratio of PI-labeled cells to the total number of cells in the field of view (FOV). As PI can only bind the DNA of cells with substantial membrane damage, a PI-labeled cell would indicate that the cell were in late apoptosis stage [31].

Statistical analysis

All experiments were performed at least in triplicates and the data was reported as mean ±SD. A p value of <0.05 was considered as statistically significant using paired Student's t test.

Results

Capturing of cells in a PDMS microwell array

The cells were captured inside the microwells using a vacuum-assisted sweeping method that was recently developed in our laboratory. Briefly, the cell capturing method utilizes a combination of vacuum degassing step to facilitate the entrance of cells into each microwell and a gentle sweeping step to remove excess cells around the microwells (Electronic supplementary material, Fig. S1). A detail schematic illustration of this cell capturing method can be found in the Electronic supplementary material. Using this method, the well occupancy was over 94 % for a 100-μm size microwell array, and each well had an average

Author Manuscript Author Manuscript Author Manuscript Author Manuscript

of five to eight cells (Electronic supplementary material, Fig. S2b). At a 4× magnification resolution, 100 microwells could be acquired within the FOV (Electronic supplementary material, Fig. S2a). Therefore, the drug response of 500–800 individual cells could be quantified within a FOV. As three images were acquired at different locations on the same microwell array for each sample, the drug response of 1,500–2,400 individual cells were quantified.

Quantification of drug response of HeLa cells in the microwell array using fluorescence imaging

HeLa cells captured in the microwell array were treated with the selected chemotherapeutic drugs, cisplatin, and paclitaxel. The drug response of individual cells in the microwell array was evaluated based on the changes in metabolic activities (i.e., uptake of 2-NBDG) in the drug-treated HeLa cells compared with the control cells. Intracellular uptake of 2-NBDG was quantified based on the fluorescence intensities of individual cells in the microwell array (Fig. 2). The representative fluorescence images of the control and cisplatin- and paclitaxel-treated HeLa cells inside a 100-μm microwell array were imaged using a 4× objective (Fig. 2a–c), and a close-up view of individual microwells for each sample was acquired using a 10× objective (Fig. 2d–f). Quantification of the mean integrated intensity of individual cells within the microwell array from the ×4 objective images was performed using the Cell Profiler software[28] (Fig. 2g). From the fluorescence images, it was visually evident that the control HeLa cells had higher fluorescence intensities compared with the drug-treated cells (Fig. 2a–f). Quantification of the integrated intensity by the Cell Profiler software showed a 30 and 49 % reduction in 2-NBDG uptake in the cisplatin- and paclitaxel-treated cells, respectively (Fig. 2g). A representative line scan analysis across a single cell (acquired using a 10× objective) was performed to demonstrate both the intracellular distribution of 2-NBDG and also illustrate the reduction in 2-NBDG uptake in the drug-treated cells compared with the control cells after 3 h of drug treatment (Electronic supplementary material, Fig. S3).

Quantification of drug response of 5637 cells in the microwell array using fluorescence imaging

To demonstrate the potential of this microwell array molecular imaging approach in quantifying drug response in diverse cancer cells, a bladder cancer cell line, 5637 was selected and assessed for drug response using the same methods as described above for the HeLa cells. The fluorescence intensity corresponding to the uptake of 2-NBDG in the control and cisplatin- and paclitaxel-treated 5637 cells inside the microwell array was quantified using the Cell Profiler software as described above (Fig. 3a–c). Image of individual microwells was also acquired using a 10× objective to show the distribution of cells within a microwell (Fig. 3d–f). The mean integrated intensity of each individual cells was determined by the Cell Profiler software and plotted (Fig. 3g). Similar to the results obtained for the HeLa cells, the fluorescent intensity corresponding to 2-NBDG uptake was visibly higher in the control 5637 cells compared with the drug-treated cells (Fig. 3a–g). The results obtained from the Cell Profiler software showed a 27 and 43 % reduction in 2-NBDG uptake in the cisplatin and paclitaxel-treated 5637 cells, respectively (Fig. 3g) after 3 h of drug treatment. The representative line scan analysis across a single cell showed that the

Author Manuscript Author Manuscript Author Manuscript Author Manuscript

intracellular uptake of 2-NBDG in the drug-treated cells was lower compared with the control cells after 3 h of drug treatment (Electronic supplementary material, Fig. S4).

Taken together, the results demonstrate that drug response of individual cancer cells for two common chemotherapy drugs (cisplatin and paclitaxel) at clinically relevant concentrations could be detected within 3 h using this current micro-array molecular imaging approach. In addition, the current approach was effective in evaluating the drug response in both bladder and cervical cancer cell lines, illustrating the potential of this approach for quantifying chemosensitivity across multiple cancers.

Flow cytomteric analysis of drug response

To quantify the 2-NBDG uptake in a larger sample population (cultured in a 6-well plate), the drug response of treated cells was compared with the control cells by flow cytometry (Fig. 4). Based on the results of flow cytometry, a significant reduction in 2-NBDG uptake was observed in the drug-treated cells compared with the control (Fig. 4). For the HeLa cells, a 22 and 27 % reduction in 2-NBDG uptake was observed when the cells were treated with cisplatin and paclitaxel, respectively (Fig. 4a). A similar trend in 2-NBDG uptake was also observed in the 5637 cells, where a 27 % (cisplatin) and 21 % (paclitaxel) reduction in 2-NBDG uptake was measured compared with the control cells (Fig. 4d).

Cell viability by MTT assay following a 24-h treatment

To validate the results of the short term intracellular 2-NBDG uptake in predicating chemosensitivity, a 24-h cell viability assay was performed in a 24-well plate (Fig. 5). Results from the 24-h MTT assay showed a 23 and 15 % reduction in cell viability for the 100-μM cisplatin-treated HeLa and 5637 cells, respectively (Fig. 5). A 60 and 45 % reduction in cell viability were observed in HeLa and 5637 cells, respectively after being treated with 1 μM paclitaxel for 24 h (Fig. 5).

Evaluation of cancer cell apoptosis by cell surface morphology and PI labeling

A time dependent analysis of cell apoptosis after drug treatment was evaluated using PI labeling of HeLa (Fig. 6) and 5637 cells (Fig. 7) in an 8-well glass chamber. As PI can only enter and bind the DNA of cells with substantial membrane damage, PI-labeled cells would be indicative of the cells having significant morphological changes and are in late apoptosis [31]. The cancer cells were treated with cisplatin or paclitaxel and stained with PI at 3 and 24 h post incubation with the selected drugs to evaluate for membrane damage. At 3 h, no significant difference in cell morphology (HeLa, Fig. 6a–c; 5637, Fig. 7a–c) or PI labeling was observed between the control and the drug-treated cells (HeLa, Fig. 6d–f; 5637, Figs. 7d–f and 8) for either cell lines. However, after 24 h of incubation with the drugs, both the cisplatin and paclitaxel-treated HeLa cells showed a 2-fold increase in PI-labeled cells compared with the control (Figs. 6j–l and 8). Similarly, the cisplatin and paclitaxel-treated 5637 cells also showed a 2- and 7.6-fold increase in PI-labeled cells, respectively compared with the control (Figs. 7j–l and 8). In addition, the drug-treated cells also exhibit substantial changes in their cell morphologies compared with the control based on brigthfield microscopic images (HeLa, Fig. 6g–i; 5637, Fig. 7g–i). Moreover, the morphological changes were more pronounced in the paclitaxel-treated cells in both cell lines, as indicated

Author Manuscript Author Manuscript Author Manuscript Author Manuscript

by the degree of cell blebbing and rounding of most of the cells (HeLa, Fig. 6i; 5637, Fig. 7i).

Discussion

In this study, a rapid and sensitive approach was developed to quantify the drug response of cancer cells using a combination of cell microarray and molecular imaging. Cancer cells were captured within each microwell in an array using a simple but effective cell capturing approach. This approach can produce microwell arrays with >90 % well occupancy and consistent cell distribution (Electronic supplementary material). In addition, the open system design used in this cell microarray study also allowed for easy fluid exchange, maintained the cells in a controlled environment (5 % CO_2 and humidified atmosphere), and provided a uniform distribution of drugs to each microwell without the need of microfluidic channels and pumps.

In the previous cancer drug response microarray studies, the efficacy of the anticancer drugs were detected based on changes in gene expression of cell surface markers such as β1-integrin [10], E-cadherin [10, 12], and NF-κB [11]. While successful, these assays typically require a 24–48 h of drug incubation before significant changes in the gene expression could be detected [10–12]. As upregulation of glycolysis is a near-universal phenomenon that has been observed across different cancers [32, 33], predictive markers based on cell metabolism such as intracellular glucose uptake may provide a better evaluation of cell viability across diverse cancer cells and in a shorter time period [17, 18]. Quantification of drug response based on 2-NBDG uptake has been shown previously in breast [17, 18], ovarian [34], liver [17], and cervical cancer cells [30]. In most of these previous studies, the drug response was measured after 24–48 h of drug treatment using 2-NBDG uptake [17, 18]. In contrast to these previous studies, the results of this study and our earlier work [30] showed that the drug response could be quantified at a much earlier time point (3 h) using two cancer cell lines (HeLa and 5637) and two anticancer drugs (cisplatin and paclitaxel) at clinically relevant drug concentrations.

A comparative analysis of the current microwell molecular imaging approach with conventional flow cytometry showed a similar reduction in the intracellular 2-NBDG uptake for the cisplatin-treated cells compared with the controls for both cancer cell lines (Figs. 2, 3, and 4). However, in both the paclitaxel-treated cells, the percentage decrease in intracellular 2-NBDG quantified by flow cytometry were lower compared with that by the microwell molecular imaging approach (Figs. 2, 3, and 4). The discrepancy in the 2-NBDG uptake in the case of the paclitaxel treatment could be attributed to both the physical and metabolic states of the cells. The cells in the microwell array were captured within each microwell after they were detached from a culture flask. The settling time of the cells in the microwell was only 30 min, which was not sufficient for the cells to spread like the cells in the 6-well plate, where they were grown for at least 24 h. As paclitaxel is a microtubule-stabilizing chemotherapy drug [22, 23], its effect may be more significant when cells are rounded (as in the case for the cells in the microwell array). Moreover, given the fact that the cells grown in a 6-well plate for flow cytometry were trypsinized after 2-NBDG uptake, the trypsinization process may also alter the metabolic state of the cells that could influence the

Author Manuscript Author Manuscript Author Manuscript Author Manuscript

flow cytometry results. Nevertheless, the results from flow cytometry confirmed that a significant decrease in 2-NBDG uptake could be detected in 3 h using the current microwell imaging approach, and as few as 1,500 cells were needed as compared with 10^6 cells used in flow cytometry.

To further evaluate the sensitivity of this short term (3 h) assay in predicting drug response of cancer cells, the percent reduction in 2-NBDG uptake was compared with the conventional MTT cell viability assay, PI staining, and cell surface morphology analysis using brightfield microscopy in a 24-h experiment (Figs. 5, 6, 7, and 8). Using these conventional cell viability assays, the drug response in both cancer cell lines and the two different anticancer drugs could only be detected after 24 h of drug treatment (Figs. 5, 6, 7, and 8). No significant changes in cell viability could be detected using either MTTor PI staining in 3 h (Figs. 5, 6, 7, and 8), nor was there a difference in cell surface morphology between the control and the drug-treated cells (Figs. 6 and 7). The smaller and brighter nuclear PI staining of the drug-treated cells after 24 h were due to nuclear chromatin condensation and DNA frag-mentation, which are the key features of apoptosis [35]. This provided further evidence that the changes in cellular glucose metabolism after a short period of drug treatment (3 h) could predict eventual cell death as determined in the longer term (24 h) conventional cell viability assay such as MTT, PI staining and cell surface morphology analysis.

Taken together, the results of this study showed that a rapid and sensitivity assay to quantify drug response in cancer cells could be achieved using a microarray molecular imaging approach. The drug response sensitivity of the current approach showed a similar trend and was comparable to the results using conventional assays: flow cytometry, MTT cell viability assay, and PI staining with cell surface morphology analysis. This combination of microwell and molecular imaging technology allows for a rapid and high-throughput screening of individual cell response with very low sample volumes requirement. Given the limitations of CSRAs and the lack of in vitro assays to predict drug response, this approach could also be translated into clinical settings where individual cells from a solid tumor could be isolated using brush, needle, or punch biopsies. The clinical samples could then be rapidly analyzed for drug response without extended culturing of the tissue sample. This microarray molecular imaging approach has great potential in cancer research to better understand drug resistance in cancer tumors and would allow for a more personalized medicine in clinical applications.

Conclusions

The microarray molecular imaging approach described here provides a rapid and sensitive method for measuring drug response of individual cells to diverse chemotherapy drugs across multiple cancers. The sensitivity of this approach was comparable to conventional flow cytometry; however only 1,000–2,000 cells are needed compared with the 10^6 cells normally needed for flow cytometry. Moreover, the drug response of individual cells was detected within 3 h after drug treatment. This detection time was significantly faster compared with the traditional cell viability assays that typically require at least 24 h. Given the sensitivity and speed of this approach in detecting drug response, it holds promise both

Author Manuscript Author Manuscript Author Manuscript Author Manuscript

as a research tool to improve the understanding of drug resistance in cancer cells and as a point-of-care platform for a more personalized treatment of cancer.

Supplementary Material

Refer to Web version on PubMed Central for supplementary material.

Acknowledgment

Support from the UC Cancer Research Coordinating Committee (3-440348-36240) is acknowledged.

References

1. Johnstone RW, Ruefli AA, Lowe SW. Apoptosis: a link between cancer genetics and chemotherapy. Cell. 2002; 108:153–164. [PubMed: 11832206]
2. Kang HC, Kim I-J, Park J-H, et al. Identification of genes with differential expression in acquired drug-resistant gastric cancer cells using high-density oligonucleotide microarrays. Clin Cancer Res. 2004; 10:272–284. [PubMed: 14734480]
3. Gottesman MM. Mechanisms of cancer drug resistance. Annu Rev Med. 2002; 53:615–627. [PubMed: 11818492]
4. Schrag D, Garewal HS, Burstein HJ, et al. American Society of Clinical Oncology Technology Assessment: chemotherapy sensitivity and resistance assays. J Clin Oncol. 2004; 22:3631–3638. [PubMed: 15289488]
5. Samson DJ, Seidenfeld J, Ziegler K, et al. Chemotherapy sensitivity and resistance assays: a systematic review. J Clin Oncol. 2004; 22:3618–3630. [PubMed: 15289487]
6. Burstein HJ, Mangu PB, Somerfield MR, et al. American Society of Clinical Oncology clinical practice guideline update on the use of chemotherapy sensitivity and resistance assays. J Clin Oncol. 2011; 29:3328–3330. [PubMed: 21788567]
7. Meacham CE, Morrison SJ. Tumour heterogeneity and cancer cell plasticity. Nature. 2013; 501:328–337. [PubMed: 24048065]
8. Fernandes TG, Diogo MM, Clark DS, et al. High-throughput cellular microarray platforms: applications in drug discovery, toxicology and stem cell research. Trends Biotechnol. 2009; 27:342–349. [PubMed: 19398140]
9. Russo G, Zegar C, Giordano A. Advantages and limitations of microarray technology in human cancer. Oncogene. 2003; 22:6497–6507. [PubMed: 14528274]
10. Meli L, Jordan ET, Clark DS, et al. Influence of a three-dimensional, microarray environment on human cell culture in drug screening systems. Biomaterials. 2012
11. Chen P-C, Huang Y-Y, Juang J-L. MEMS microwell and microcolumn arrays: novel methods for high-throughput cell-based assays. Lab Chip. 2011; 11:3619–3625. [PubMed: 21904742]
12. Håkanson M, Kobel S, Lutolf MP, et al. Controlled breast cancer microarrays for the deconvolution of cellular multilayering and density effects upon drug responses. PloS ONE. 2012; 7:e40141. [PubMed: 22792141]
13. Kwon CH, Wheeldon I, Kachouie NN, et al. Drug-eluting microarrays for cell-based screening of chemical-induced apoptosis. Anal Chem. 2011; 83:4118–4125. [PubMed: 21476591]
14. Fletcher JW, Djulbegovic B, Soares HP, et al. Recommendations on the use of 18F-FDG PET in oncology. J Nucl Med. 2008; 49:480–508. [PubMed: 18287273]
15. Hsu PP, Sabatini DM. Cancer cell metabolism: Warburg and beyond. Cell. 2008; 134:703–707. [PubMed: 18775299]
16. Vander Heiden MG, Cantley LC, Thompson CB. Understanding the Warburg effect: the metabolic requirements of cell proliferation. Science. 2009; 324:1029–1033. [PubMed: 19460998]
17. O'neil RG, Wu L, Mullani N. Uptake of a fluorescent deoxyglucose analog (2-NBDG) in tumor cells. Mol Imaging Biol. 2005; 7:388–392. [PubMed: 16284704]

Author Manuscript Author Manuscript Author Manuscript Author Manuscript

18. Millon SR, Ostrander JH, Brown JQ, et al. Uptake of 2-NBDG as a method to monitor therapy response in breast cancer cell lines. Breast Cancer Res Treat. 2011; 126:55–62. [PubMed: 20390344]
19. Siddik ZH. Cisplatin: mode of cytotoxic action and molecular basis of resistance. Oncogene. 2003; 22:7265–7279. [PubMed: 14576837]
20. Liebmann J, Cook J, Lipschultz C, et al. Cytotoxic studies of paclitaxel (Taxol) in human tumour cell lines. Br J Cancer. 1993; 68:1104. [PubMed: 7903152]
21. Fuertes MA, Alonso C, Pérez JM. Biochemical modulation of cisplatin mechanisms of action: enhancement of antitumor activity and circumvention of drug resistance. Chem Rev. 2003; 103:645–662. [PubMed: 12630848]
22. Kumar N. Taxol-induced polymerization of purified tubulin. Mechanism of action. J Biol Chem. 1981; 256:10435–10441. [PubMed: 6116707]
23. Horwitz SB, Cohen D, Rao S, et al. Taxol: mechanisms of action and resistance. Je Natl Cancer Inst. Monographs. 1993; 55
24. Rettig JR, Folch A. Large-scale single-cell trapping and imaging using microwell arrays. Anal Chem. 2005; 77:5628–5634. [PubMed: 16131075]
25. Malinin TI, Perry VP. Toxicity of dimethyl sulfoxide on HeLa cells. Cryobiology. 1967; 4:90–96. [PubMed: 4171657]
26. Rassouli FB, Matin MM, Iranshahi M, et al. Investigating the enhancement of cisplatin cytotoxicity on 5637 cells by combination with mogoltacin. Toxicol In Vitro. 2011; 25:469–474. [PubMed: 21126568]
27. Gibb RK, Taylor DD, Wan T, et al. Apoptosis as a measure of chemosensitivity to cisplatin and taxol therapy in ovarian cancer cell lines. Gynecol Oncol. 1997; 65:13–22. [PubMed: 9103385]
28. Lamprecht MR, Sabatini DM, Carpenter AE. Cell Profiler™: free, versatile software for automated biological image analysis. Biotechniques. 2007; 42:71. [PubMed: 17269487]
29. Carmichael J, Mitchell J, Degraff W, et al. Chemosensitivity testing of human lung cancer cell lines using the MTT assay. Br J Cancer. 1988; 57:540. [PubMed: 2841961]
30. Luo Z, Tikekar RV, Samadzadeh KM, et al. Optical molecular imaging approach for rapid assessment of response of individual cancer cells to chemotherapy. J Biomed Opt. 2012; 17:1060061–1060068.
31. Vitale M, Zamai L, Mazzotti G, et al. Differential kinetics of propidium iodide uptake in apoptotic and necrotic thymocytes. Histochemistry. 1993; 100:223–229. [PubMed: 8244773]
32. Gillies RJ, Robey I, Gatenby RA. Causes and consequences of increased glucose metabolism of cancers. J Nucl Med. 2008; 49:24S–42S. [PubMed: 18523064]
33. Gatenby RA, Gillies RJ. Why do cancers have high aerobic glycolysis? Nat Rev Cancer. 2004; 4:891–899. [PubMed: 15516961]
34. Egawa-Takata T, Endo H, Fujita M, et al. Early reduction of glucose uptake after cisplatin treatment is a marker of cisplatin sensitivity in ovarian cancer. Cancer Sci. 2010; 101:2171–2178. [PubMed: 20678156]
35. Bonfoco E, Krainc D, Ankarcrona M, et al. Apoptosis and necrosis: two distinct events induced, respectively, by mild and intense insults with N-methyl-D-aspartate or nitric oxide/superoxide in cortical cell cultures. Proc Natl Acad Sci. 1995; 92:7162–7166. [PubMed: 7638161]

Author Manuscript Author Manuscript Author Manuscript Author Manuscript

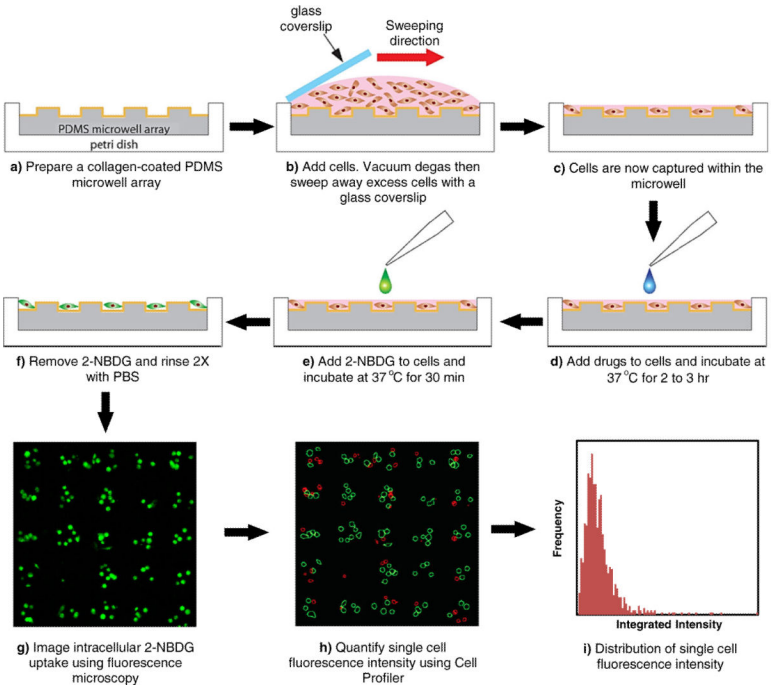

Fig. 1.

Schematic illustration of the microwell molecular imaging approach for single cell analysis. **a** The cell microarray consists of a 100-μm PDMS microwell array that was affixed to a Petri dish. **b** Cells were captured inside the microwell using a two-step process. First, cells were placed on a collagen-coated PDMS microwell array and vacuum degassed to facilitate entry of cells into the microwells. After a period of 30 min to allow the cells to attach to the microwell, the excess cells on the outside of the microwells were swept away using a glass coverslip. **c** The microwells were rinsed and ready for use. **d** Known concentrations of drugs were pipetted directly into the microwell array inside the Petri dish and incubated for 2 to 3 h. **e** 2-NBDG was added to the cells in the microwells and incubated for another 30 min to allow uptake of the glucose analog. **f** The media were removed, and the microwells were rinsed once with PBS. **g** The image of the cell microarray was captured using fluorescence microscopy. **h, i** The fluorescence intensities of individual cells were quantified using Cell Profiler and analyzed. Note: Figure is not drawn to scale

Author Manuscript Author Manuscript Author Manuscript Author Manuscript

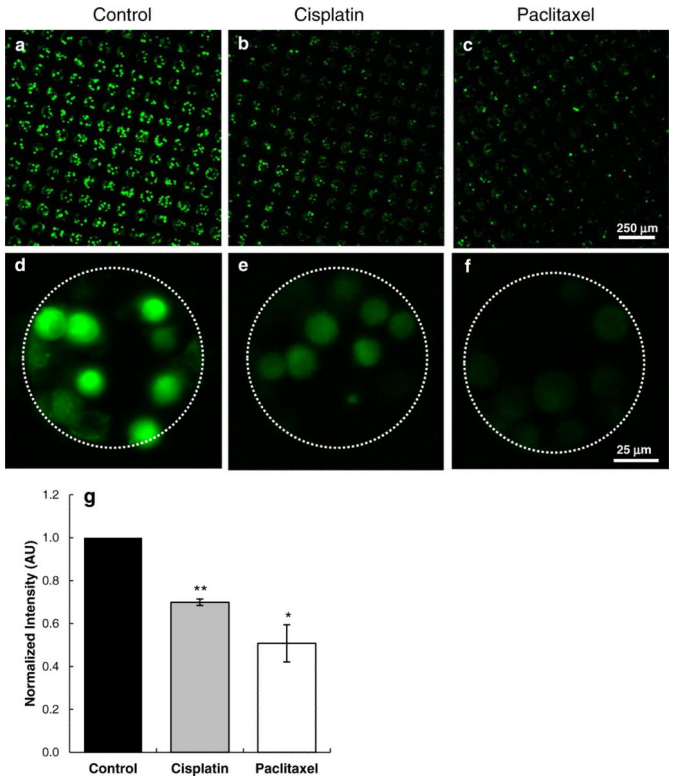

Fig. 2.

Quantification of drug response of the HeLa cells in the microwell array using molecular imaging. **a–c** Representative fluorescence images (using a 4× objective) of the HeLa cells after 3 h of drug treatment with cisplatin or paclitaxel. **d–f** Higher magnification (10× objective) images showing a close-up view of cells inside one microwell (*white dotted circle*). **g** Normalized integrated intensities of the 2-NBDG uptake in the control and drug-treated HeLa cells. Mean±standard deviation, N=3. *p<0.05; **p<0.01, compared with control

Author Manuscript Author Manuscript Author Manuscript Author Manuscript

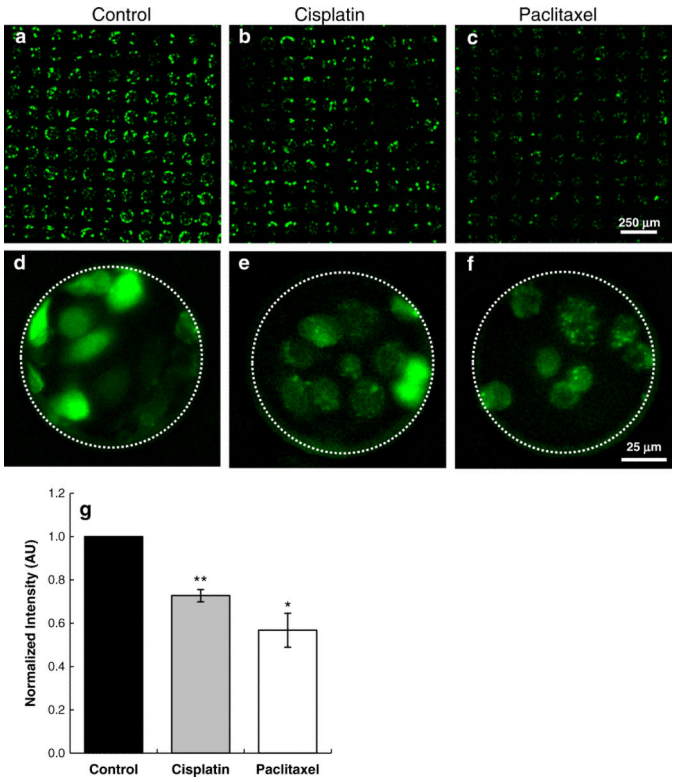

Fig. 3.

Quantification of drug response of 5637 bladder cancer cells in the microwell array using molecular imaging. **a–c** Representative fluorescence images of 5,637 cells after 3 h of drug treatment with cisplatin or paclitaxel (4× objective). **d–f** Higher magnification (10× objective) images showing a close-up view of cells inside one microwell (*white dotted circle*). **g** Normalized integrated intensities of the 2-NBDG uptake in the control and drug-treated 5,637 cells. Mean±standard deviation, N=3. *p<0.05; **p<0.01, compared with control

Author Manuscript Author Manuscript Author Manuscript Author Manuscript

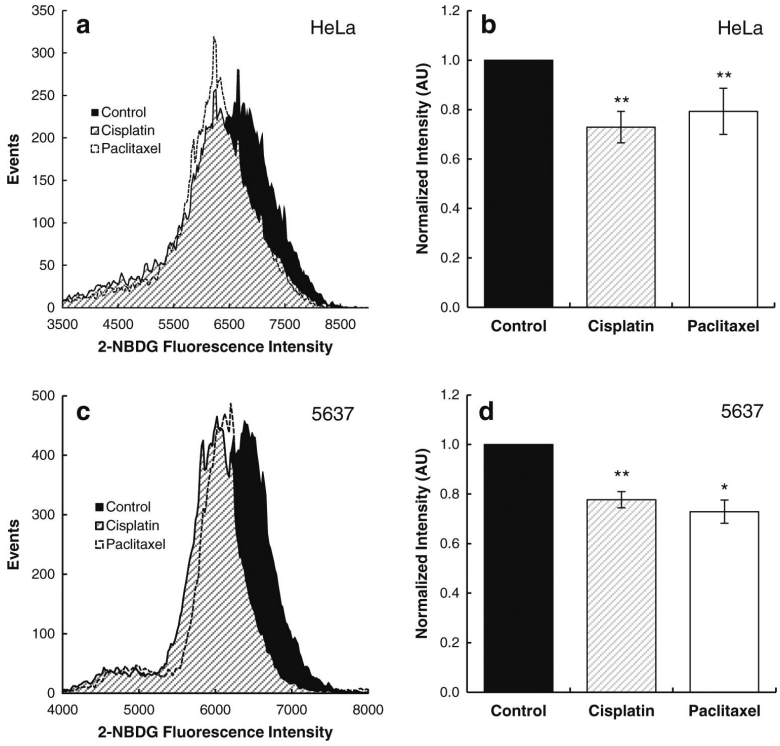

Fig. 4.

Flow cytometric analyses of 2-NBDG uptake by **(a, b)** HeLa and **(c, d)** 5637 cells. The histograms **(a, c)** display the distribution of fluorescence intensities for each cell lines, and the *bar graphs* **(b, d)** show the normalized fluorescence intensity corresponding to 2-NBDG uptake in the drug-treated and control cells for both cell lines. Mean±standard deviation, N=3. **p<0.01; *p<0.05, compared with control

Author Manuscript Author Manuscript Author Manuscript Author Manuscript

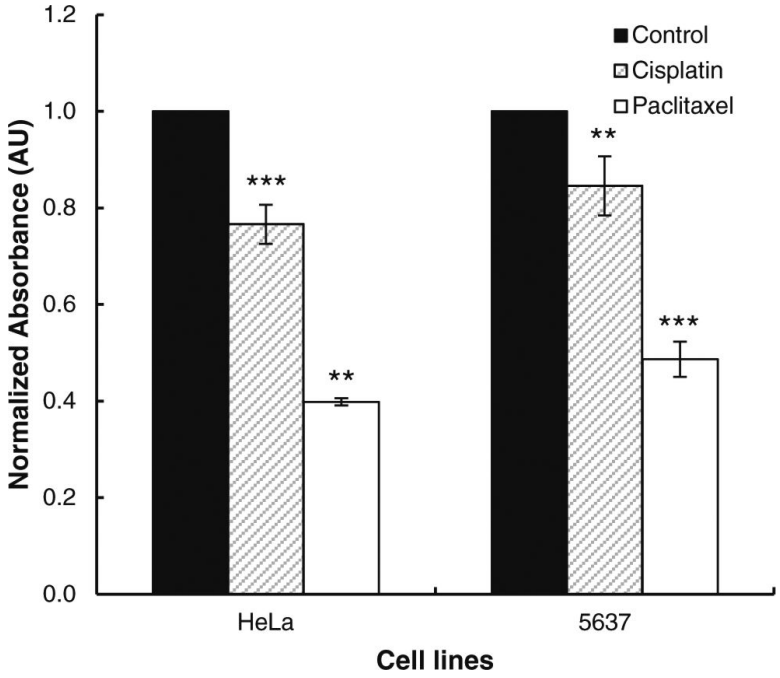

Fig. 5.

Cell viability after 24 h of drug treatment by the MTT assay. *Bar graphs* represent the normalized UV/vis absorbance measured at 540 nm in **a** cisplatin- and **b** paclitaxel-treated cells for both HeLa and 5637 cell lines. Mean±standard deviation, N=3. **p<0.01; ***p<0.001, compared with control

Author Manuscript Author Manuscript Author Manuscript Author Manuscript

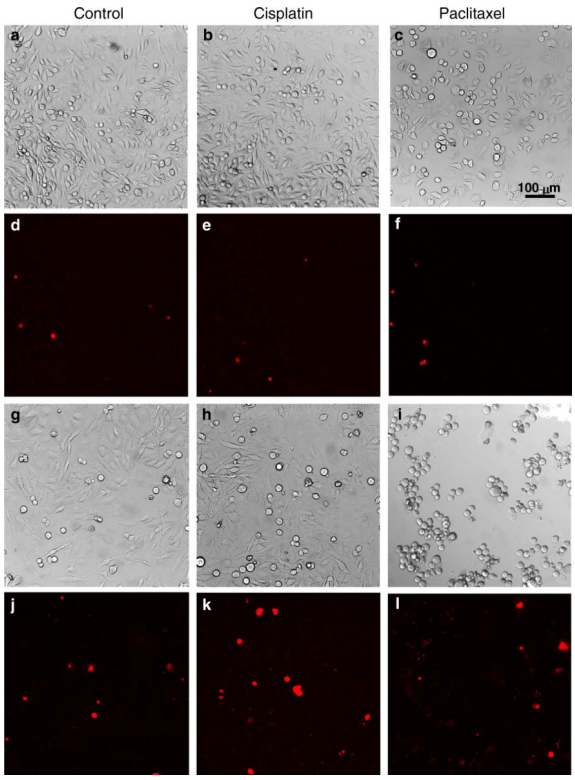

Fig. 6.

Changes in cell morphology by brightfield microscopy and membrane permeability by PI staining induced by drug treatment in the HeLa cells. Representative brightfield and fluorescence images of the HeLa cells after **a–f** 3 and **g–)** 24 h of drug treatment. The nuclei of cells with compromised membrane are labeled by PI (*red*)

Author Manuscript Author Manuscript Author Manuscript Author Manuscript

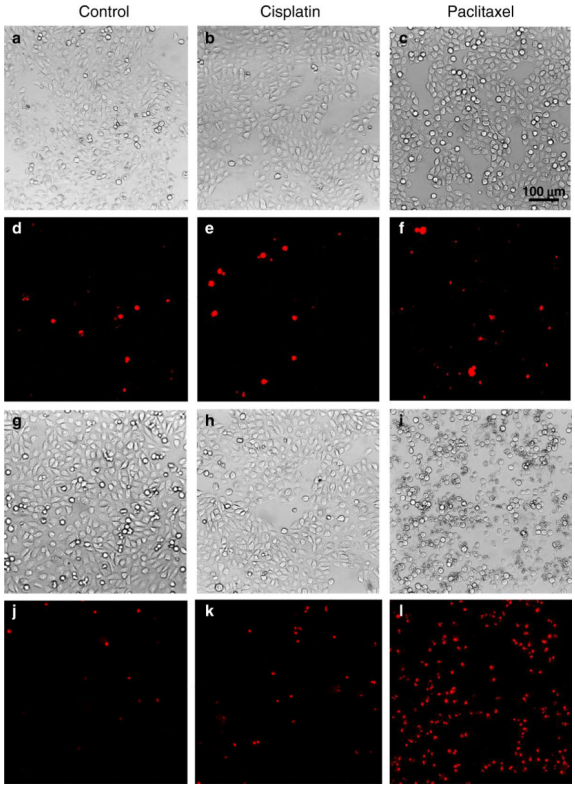

Fig. 7.

Monitoring changes in cell morphology by brightfield microscopy and membrane permeability by PI staining induced by drug treatment in the 5637 cells. Representative brightfield and fluorescence images of the 5637 cells after **a–f** 3 and **g–l** 24 h of drug treatment. The nuclei of cells with compromised membrane are labeled by PI (*red*)

Author Manuscript Author Manuscript Author Manuscript Author Manuscript

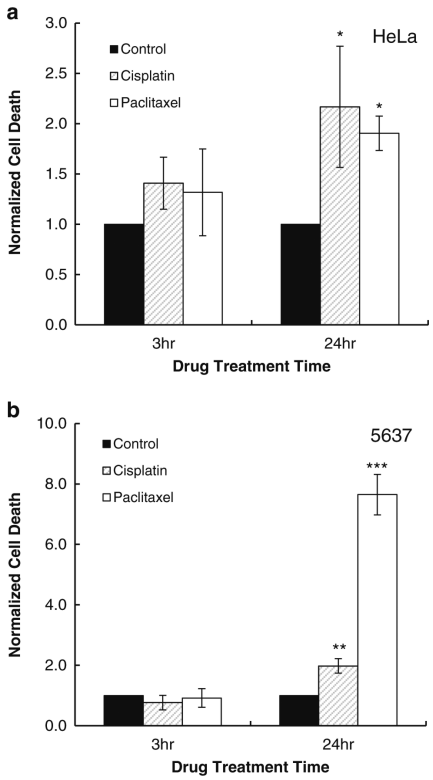

Fig. 8.

Quantification of PI-labeled HeLa and 5637 cells after 3 and 24 h of drug treatment with 100 μM cisplatin or 1 μM paclitaxel. The percent cell death was determined by the ratio of PI-labeled cells to the total number of cells and normalized to the control. Data represent mean±SD, N=3. *p<0.05; **p<0.01; ***p<0.001